UNIVERSITY OF CALIFORNIA,

IRVINE

Saliva based Electrochemical detection for diagnosis of malaria

THESIS

submitted in partial satisfaction of the requirements

for the degree of

MASTER OF SCIENCE

in Electrical Engineering

by

Yuanhang Li

Thesis Committee:

Professor William C. Tang, Chair

Professor Peter J. Burke

Professor Pai H. Chou

2016

DEDICATION

To

My father

Mr. BAO LI

Who is always supportive.

My mother

Mrs. LIFANG CAO

who is always open-minded.

TABLE OF CONTENTS

LIST OF FIGURES

LIST OF TABLES

ACKNOWLEDGMENTS

I would like to express the deepest appreciation to my committee chair, Professor William C. Tang, who gives me a lots of opportunities to work on different projects and learn various things. Without his creativity, guidance and persistent help this thesis would not have been possible.

I would like to thank my committee members, Professor Peter J. Burke and Professor Pai H. Chou, whose are willing to spare their precious time and be my committee members.

In addition, a big thank you to Dr. Ting-Hsuan CHEN of City University of Hong Kong, who supervised my first research project and provided invaluable help.

Finally, I would like to express my profound gratitude to my father, Mr. Bao LI and my mother, Mrs. Lifang CAO who have been supportive all the time. I deeply realize that I cannot achieve anything without their unconditional love and sacrifice.

ABSTRACT OF THE THESIS

Saliva based Electrochemical detection for diagnosis of malaria

By

Yuanhang Li

Master of Science in Electrical Engineering

University of California, Irvine, 2016

Professor William C. Tang, Chair

Rapid Diagnostic tests (RDTs) products for malaria available on market today are all blood-based. Massive research have been done to find a cheap and convenient method to diagnose malaria using saliva samples. In this project, an innovative approach by converting electrochemical impedance change to voltage difference variation was demonstrated. Through the functionalization of Au electrode surface with pLDH aptamers and construction of Wheatstone bridge using interdigitated electrodes, a significant voltage difference was measured which showed potential for not only qualitative but also for quantitative detection of malaria utilizing saliva specimen. An electrical circuit prototype was also assembled demonstrating the feasibility of making a portable device for measurement.

CHAPTER 1: INTRODUCTION

1.1 Burden of malaria on undeveloped counties

Malaria is a mosquito-borne infectious disease caused by parasites belonging to the genus Plasmodium. There are five species of parasites that can cause malaria in human and four of these (Plasmodium vivax, Plasmodium falciparum, Plasmodium ovale and Plasmodium malariae) can spread among people via the bite of female Anopheles mosquitoes while Plasmodium knowlesi infects human through zoonotic transmission [1]. Plasmodium vivax and Plasmodium falciparum are the most challenging threat to public health. Plasmodium vivax has a very wide distribution over the planet since it is capable of surviving and developing at lower temperatures and high altitudes. Plasmodium falciparum is prevalent in Africa which leads to most deaths of malaria.

Table 1.1 Malaria cases and deaths in different regions, 2000-2015 [1].

	Estimated number of malaria cases (000's)				Change	Estimated number of malaria deaths				Change
WHO region	**2000**	**2005**	**2010**	**2015**	**2000–2015**	**2000**	**2005**	**2010**	**2015**	**2000–2015**
African	214 000	217 000	209 000	188 000	-12%	764 000	670 000	499 000	395 000	-48%
Americas	2 500	1 800	1 100	660	-74%	1 600	1 200	1 100	500	-69%
Eastern Mediterranean	9 100	8 600	4 000	3 900	-57%	15 000	15 000	7 000	7 000	-51%
European*	36	5.6	0.2	0	-100%	0	0	0	0	
South-East Asia	33 000	34 000	28 000	20 000	-39%	51 000	48 000	44 000	32 000	-37%
Western Pacific	3 700	2 300	1 700	1 500	-59%	8 100	4 200	3 500	3 200	-60%
World	**262 000**	**264 000**	**243 000**	**214 000**	**-18%**	**839 000**	**738 000**	**554 000**	**438 000**	**-48%**
Lower bound	205 000	203 000	190 000	149 000		653 000	522 000	362 000	236 000	
Upper bound	316 000	313 000	285 000	303 000		1 099 000	961 000	741 000	635 000	

Through years of efforts, malaria infection has reduced by 37% and the risk of dying due to malaria has decreased by 60%. However, millions of people are still suffering from malaria or potentially have risks. It was estimated that the number of malaria infections was 214 million with 438,000 of them died in 2015 [Table 1.1]. Most of the infections occur in undeveloped countries in Africa (88%) and South-East Asia (10%).

1.2 Significance and motivation

Malaria as a public health issue exhibits financially and socially significant influence. In order to control malaria, global investments increased from 960 million USD in 2005 to 2.5 billion in 2014. However, despite the intensive investment, millions of people are still unable to receive the needed service. Solely in sub-Saharan Africa in 2014, it was estimated that around 269 million people at risk of malaria lived in households without a single Insecticide-treated bed nets or indoor residual spraying; 15 million pregnant women at risk couldn't receive a single dose of intermittent preventive treatment in pregnancy and between 68 and 80 million children with malaria did not receive Artemisinin-based Combination Therapy. Socially, malaria attacks bring burdens on families making them much more fragile and children suffering cerebral malaria could have brain damage which has impaired their learning abilities [2]. Therefore, convenient and cheap malaria diagnosis products have been badly needed to lower the financial burden and control malaria infection.

1.3 Current methods for malaria diagnosis

Doctors with knowledge and experience can directly do clinical diagnosis based on patients' symptoms. But it is imprecise since the symptoms could overlap with other tropical diseases. However, clinical diagnosis remains the major methods in endemic areas where modern medical facilities are out of reach. Biological diagnosis available commercially is blood-based, which has two main approaches.

1.3.1 Giemsa microscopy

Since the introduction of a mixture of eosin stains and methylene by Gustav Giemsa in 1904, malaria can have been diagnosed by examining Giemsa-stained blood smears under microscope which has become the standard approach [3]. Although it is very cheap to perform microscopy, the images obtained are sufficient to help doctors quantify and differentiate parasites. However, well-trained and experienced microscopists are needed for such tests to ensure effective quality. For sensitivity, Giemsa-stained thick blood film has an estimated detection threshold of 4–20 parasites/mcL [4]. To identify parasites species, it is necessary to check morphologic, differential-diagnostic details inside the thin film. Important factors include erythrocyte size, color, shape, characteristic dots, pigment structure and so on. But frequent failure exists even to differentiate the two most common species Plasmodium falciparum from Plasmodium vivax in routine microscopy. The effort to estimate parasite density could also have errors especially in low parasite density cases. Moreover, parasites may be washed off or lysed during Giemsa staining which underestimates the true parasite density [5]. Therefore,

microscopic check for malaria parasites can be unreliable and ineffective under certain circumstances.

1.3.2 Rapid Diagnostic Tests (RDTs)

Rapid diagnostic test generally requires a small amount of blood (5–15 µL) of which the result can be obtained as colored test line in 5 to 20 min. Most commercially available RDTs products are test strips that detect malaria with monoclonal antibodies directed against the target parasite antigen. RDTs test strips are easy to use without the need for long term training, maintenance, extra equipment and electricity. Different combinations of target antigens are manufactured to suit various regions among which two antigens Histidine-Rich Protein 2 (HRP-2) and Parasite lactate dehydrogenase (pLDH) are the most commonly used. HRP-2 is specific for Plasmodium falciparum while pLDH can target Plasmodium falciparum, Plasmodium vivax and Plasmodium spp. However, unlike HRP-2, pLDH doesn't persist in patient's blood for weeks making it seem to be a more appropriate target for treatment monitoring [6]. What is more, pLDH test for malaria diagnosis must first clear the existence of the asexual parasite forms since plasmodial gametocytes also produce pLDH [7]. RDTs must achieve sensitivity of at least 95% before being considered as useful tools, which is accomplished for Plasmodium falciparum detection, but not for non-Plasmodium falciparum. The detection sensitivity of RDTs is much lower than microscopy which hardly works when parasite density is less than 500/mcL blood for Plasmodium falciparum and 5,000/mcL blood for Plasmodium vivax. But in remote areas of developing countries where good microscopy services cannot be reached and no electricity, health workers with little training or supervision inevitably use RDTs for quick tests. Therefore,

as is shown in Figure 1.1, RDTs take over 60% market share of malaria diagnosis in Africa and continue to grow.

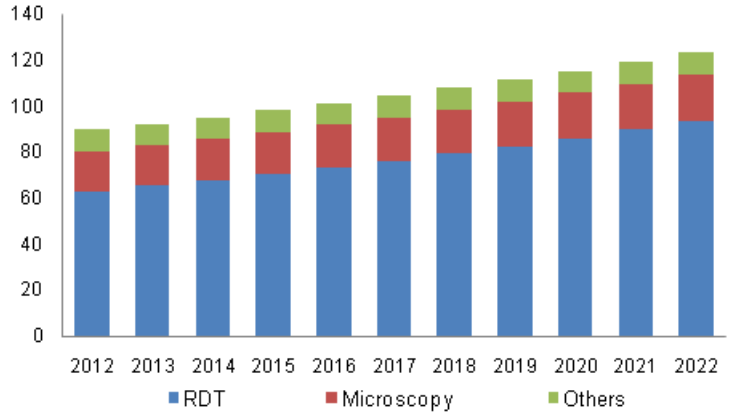

Figure 1.1 Malaria diagnosis market in Africa by technology, 2012-2022 (USD Million) [8].

1.4 Saliva based diagnosis

Saliva, composed of a complex mixture of organic and inorganic secretory products, is one of the most important body fluids found in the oral cavity. It is easy and non-invasive to obtain supplying a large range of physiological needs. A thin layer of epithelial cells separate the salivary ducts from the systemic circulation and therefore diffusion through the membrane via a passive process or against a concentration gradient can transfer substances to the saliva through active carriage. Such an exchange of substances with the plasmatic liquid makes saliva qualified as diagnosis specimen [9].

Currently, all commercial products for malaria diagnosis are blood-based and none can do malaria detection using saliva. However, drawing blood increases the risks of accidental

infections of other diseases especially in poor remote areas and people with blood taboos cannot accept blood drawing. Therefore, saliva as an easily collated and non-invasive test sample is needed. Lots of researches have been done to test different approaches utilizing saliva as diagnosis specimen. There are mainly two categories to detect malaria either by antigen or PCR. Plasmodium falciparum histidine-rich protein II (PfHRP II) was studied as the target antigen for malaria detection and evaluated by ELISA. It achieved a 100% specificity but only 43% sensitivity [10]. Further research showed that with saliva samples stabilized with protease inhibitors, sensitivities could be increased to 100% [11]. Plasmodium falciparum lactate dehydrogenase (pLDH) was also tested in saliva using OptiMAL-IT dipsticks which achieved sensitivities of 77.9% in whole saliva and 48.4% in saliva supernatant [12]. PCR method was demonstrated capable of detecting Plasmodium falciparum in human urine and saliva [13]. PCR is extremely sensitive, with a detection limit of <10 parasites/μL while the detection limit of antigen-based method is >200 parasites/μL [14, 15]. However, PCR methods are not suitable for routine point-of-care diagnosis especially in endemic regions where conditions are poor and electricity cannot be accessed. PCR requires high initial setup costs and specialized, temperature-labile consumables, which makes it impossible to be small and portable. To do PCR diagnosis, people need to take extensive trainings and experiences are necessary to ensure the reliability of test results.

1.5 Chapter summary

Malaria is still a threatening disease torturing millions of people and causing hundreds of thousands of death each year. It not only does a great damage financially to local economy but

also breaks families and leaves sequela to covered patients resulting in big social issues. Current diagnosis methods are all blood based which include microscopy and Rapid Diagnostic Tests. Microscopy is the gold standard but it still cannot eliminate errors and is limited to perform in endemic areas. Therefore, Rapid Diagnostic Tests (RDTs) start to dominate the malaria diagnosis market even though its sensitivity is lower than microscopy. However, blood drawing can be a problem since it may lead to other infections and people with blood taboos would not accept it. Hence, saliva will become the ideal test specimens, which is easily collated and non-invasive. Antigen and PCR methods were utilized by researchers to detect malaria in saliva, but they all have their own limitations and none can be commercialized.

CHAPTER 2: DETECTION APPROACH

2.1 Electrochemical impedance spectroscopy

Electrochemical impedance spectroscopy (EIS) has been studied for more than 100 years as a powerful tool for investigating the properties of electrodes and materials. It is a linear technique that can collect impedance information independent of the physical processes involved from linear electrical response systems with extraordinarily high experimental efficiency [16]. But its potential is limited since EIS requires expensive equipment.

2.1.1 Introduction to EIS

The electrochemical reaction at an electrified interface can be described as equation (1) below where **O** stands for oxidant, **n** is number of electrons transferred and **R** is its reductant.

$$\mathbf{O} + \mathbf{n}e- \longrightarrow \mathbf{R} \quad (1)$$

Figure 2.1(a-b) illustrates the electron transfer across the electrochemical interface which forms both faradaic and non-faradaic components and the electrical equivalent circuits (EECs). The faradaic components are consist of polarization resistance R_p and uncompensated solution resistance R_s. Chemicals at the interface can be modeled as double-layer capacitor C_d which is the non-faradaic component. The rate of electron transfer is determined by the mass transports of the reactant and product which is the consumption of the oxidants and the production of the reductant near the electrode surface. This mass transport leads to another class of impedance Z_W [17].

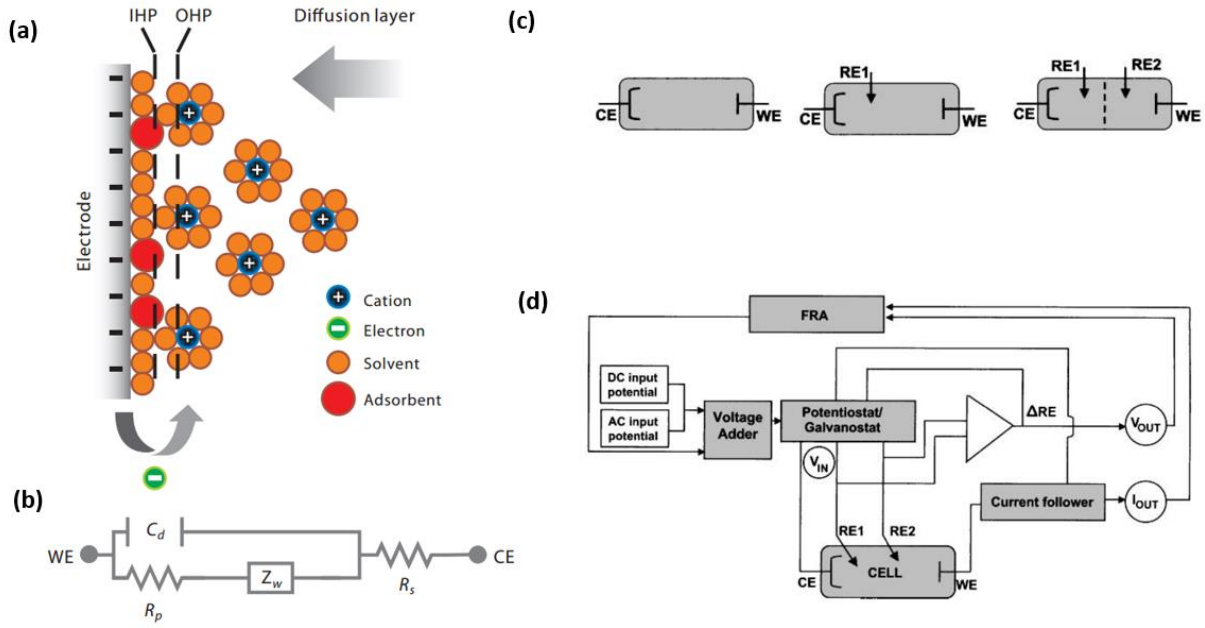

Figure 2.1: (a) Diagram of the electrified interface and its (b) electrical equivalent circuits [16]. (c) Three commonly used electrodes setup for electrochemical cells. (d) Block diagram of impedance measurement setup [17].

There are three types of electrochemical cell setup depending on the number and configuration of electrodes as are shown in Figure 2.1(c). A working electrode (WE) is where the electrochemical interface locates. Counter electrode (CE) is placed to form closed circuit allowing current flow between WE and CE. A typical CE is made of noble metal with a large surface area to stop the production of electroactive species by electrolysis that may interfere with reactions at WE. More importantly, CE with a large surface-area has high capacitance and very low impedance which can be ignored in the data of measured impedance. When there are needs to control potential difference across the electrochemical interface, one or two non-polarizable reference electrodes (RE) with constant potential can be applied in the setup [18]. The two-electrode configuration combines the function of working and reference electrode to a single WE and CE serves as the combination of counter electrode and second reference electrode. To

measure highly resistive materials where control of DC potential is not needed, two electrode setup can be chose for its convenience and accuracy. But two electrode configuration suffers the low-frequency interfacial polarization effects at the WE. Therefore, the three electrode setup is the standard for EIS measurement. The function of RE is to monitor the relative potential at the WE and it is preferred to minimize the media impedance between RE and WE by placing them close to each other. Figure 2.1(d) shows a typical setup to do EIS measurement of four electrode cell that the system measures and amplifies the voltage difference between WE and RE, and the current at the WE and then feeds the signal to the frequency response analyzer (FRA).

2.1.2 Application of EIS as biosensor

EID has been intensively researched as a label-free biosensor which shows very promising potential. The mechanism of EIS biosensor is that analyte can selectively modulate the electron transfer rate of functionalized electrode. Generally, self-assembled monolayers (SAMs) are formed to functionalize metal surfaces using the Langmuir-Blodgett method which is a spontaneous reaction with alkanethiol [19]. Functionalized electrode surface with SAMs groups can selectively capture specific analytes which intervene charge transfer rate or change the capacitance at the electrochemical interface. The charge transfer rate is also largely determined by how well the metal surface is block which is categorized by the pinholes and defects of SAMs [20]. Altered electrical properties by captured analytes can be detected by impedometric measurements and do not have to be labeled like the fluorometric method of detection. To achieve better sensitivity during the measurement, a redox probe is needed to monitor electrons

transfer at the electrochemical interface and commonly used probes include $Fe(CN)_6^{3-/4-}$, $Ru(NH_3)_6^{3+/2+}$ and p-benzoquinone/hydroquinone redox pair. Analysis of interfacial capacitance change can be constructed for proteins, DNA and heavy metal ions detection, but measurement of charge transfer rate generally show greater sensitivity [21]. Sensors for various proteins, such as p53 protein [22] and myelin basic protein [23], have been constructed through covalent conjugation of antibodies with SAMs or polyaniline film and even large analytes can be detected/monitored through EIS such as bacteria [24] and cell deaths [25]. EIS also proves itself as a good method for DNA detection since hybridization of single-stranded DNA functionalized electrode with target DNA leads to a much more crowded surface and thereby a change in electrical properties [26].

2.2 pLDH aptamer as probe

Aptamers or nucleic acid ligands are single-stranded oligonucleotide or peptide molecules that bind to a specific target molecule. Aptamers have excellent specificity and affinity for a given protein that can be used to inhibit the activity of pathogenic proteins and potentially show wide applications in clinical treatment [27]. For malaria diagnosis, pLDH aptamers can be used to detect both Plasmodium vivax LDH (PvLDH) and Plasmodium falciparum LDH (PfLDH) with strong affinities to the targets compared to pLDH antibodies. Fig 2.2(a) shows the sequence and secondary structures of two pLDH aptamers pL1 and pL2. Sensitivity of pL1 aptamer are 38.7 ± 1.3 nM and 16.8 ± 0.6 nM for PfLDH and PvLDH. For pL2 aptamer, the sensitivity for PvLDH and

PfLDH are 31.7 ± 1.6 nM and 49.6 ± 1.4 nM. The thermal stability of pLDH aptamers is good enough for most tropical environment that the melting temperatures of the pL1 and pL2 are 51.3 ˚C and 53.1 ˚C respectively. 5'-thiol-modified aptamers can be immobilized onto the gold electrode surface by simply dipping the metal into aptamers solution for 14 h [28]. When pLDH protein is bond to the aptamer creating a complex layer, the electron transport is interrupted and therefore leads to a change in impedance. Fig 2.2(c) presents the Nyquist plots of bare gold and functionalized electrode interacting with different pLDH concentration where R_{ct} is the charge transfer resistance. The value of R_{ct} is linearly proportional to both pLDH concentration and parasites density in blood on a log scale (Fig.2.2c-d) which demonstrate a possibility for quantified malaria detection.

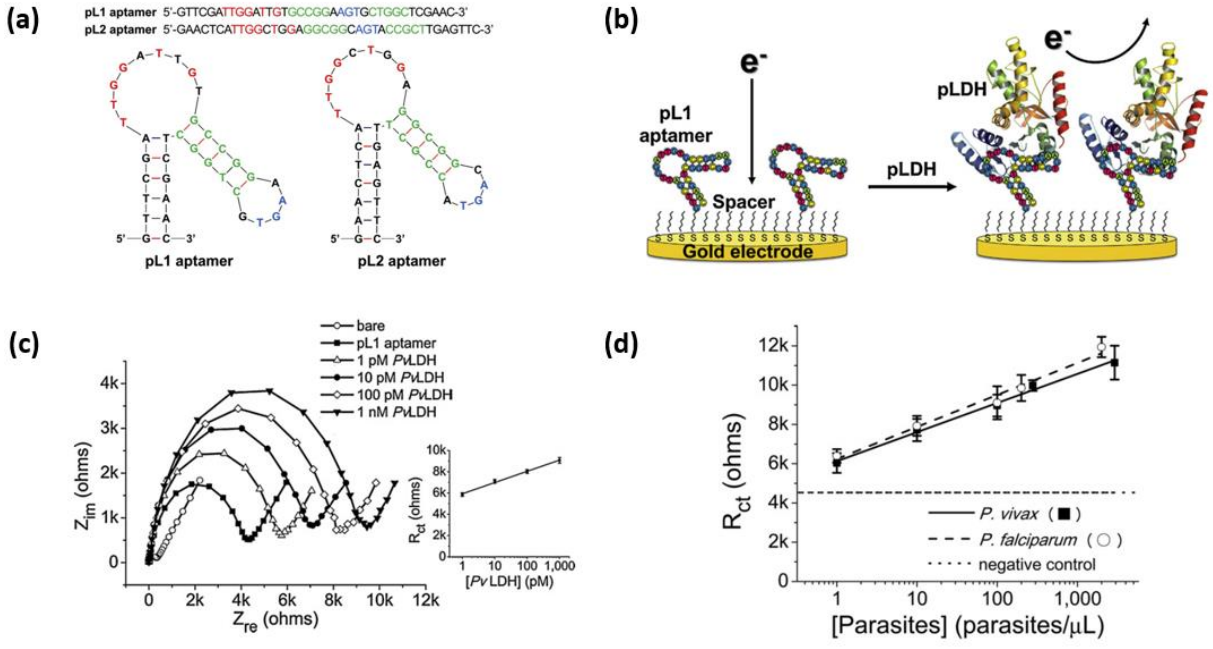

Fig 2.2: (a) Sequences and secondary structures of the pLDH aptamers: pL1 and pL2 (b) Schematic illustration for detection of pLDH proteins (c) Nyquist plots for the electrochemical detection of PvLDH using pL1 aptamer (d) Relation between R_{ct} and parasites density in blood [28].

2.3 Wheatstone bridge

Wheatstone bridge is widely known as electrical bridge circuit for the measurement of unknown resistance as shown in Fig 2.3a [29]. Resistance of R_1, R_2 and R_3 are known while R_x has unknown resistance. Resistance of R_2 is adjustable and if $R_1/R_2 = R_3/R_x$, then voltage difference between V_1 and V_2 is zero. Therefore, the resistance of R_x can be calculated as $R_x = R_2 R_3 / R_1$ by adjusting R_2 until $V_1 - V_2$ is zero.

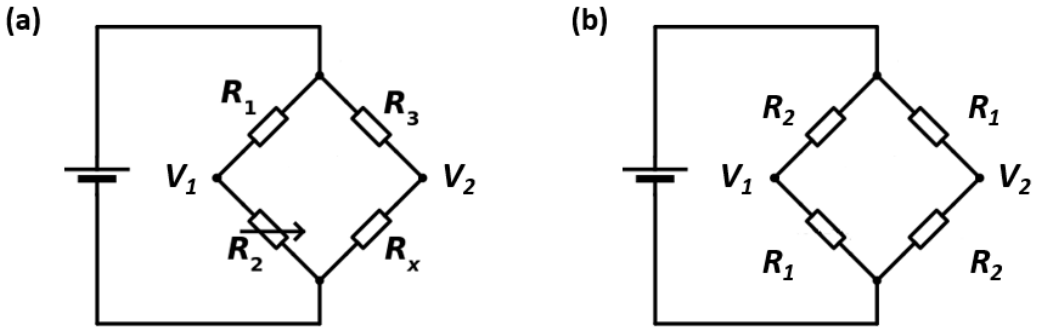

Fig 2.3: (a) Wheatstone bridge configuration used to measure unknown resistance. (b) Application of Wheatstone bridge for differential measurement.

Wheatstone bridge is practically used for differential measurement much more often in various kinds of sensors. A simplified model is illustrated in Fig 2.3(b) where there are only two resistances for four resistors. Initially, the resistance of four resistors are the same as R_0 and then outside impact (pressure, acceleration and so on) will exert equally to two R_2 causing a change in resistance which makes two R_2 increase to $R_0 + \Delta R$. The change in resistance will lead to a change in voltage which can be measured as the differential voltage V_{signal}. Similarly, the Wheatstone bridge can be configured for capacitors to do capacitive sensing. The advantage of Wheatstone

bridge is that it cancels the DC offset, effect of temperature variation and output is not dependent on absolute resistance/capacitance.

$$V_{signal} = V_2 - V_1 = \frac{\Delta R}{2R_0 + \Delta R} V \quad (2)$$

2.4 Chapter summary

Electrochemical impedance spectroscopy (EIS) is a powerful detection method of which the rudimentary mechanism is that the analyte modulate the electron transfer rate at the electrochemical interface and thereby leads to a change in electrical properties. The application of EIS is not limited to chemical analysis, which also shows great sensitivity as biosensors to detect various kinds of protein, DNA and even cells. However, common EIS requires expensive and heavy equipment with complex setup and indirect experimental data. Therefore, Wheatstone bridge which is extensively applied in sensors comes up as a promising design that can transfer electrochemical impedance to voltage.

CHAPTER 3: SENSOR AND CIRCUIT DESIGN

3.1 Design overview

Electrochemical impedance spectroscopy (EIS) demonstrates itself a great method for various detections. The idea of measuring the electrochemical impedance change, however is limited by the equipment and conventional thought. In this project, electrochemical impedance will be utilized as a part of Wheatstone bridge to convert impedance variation to voltage difference, which requires a much less complex circuit and potentially reduces size and cost.

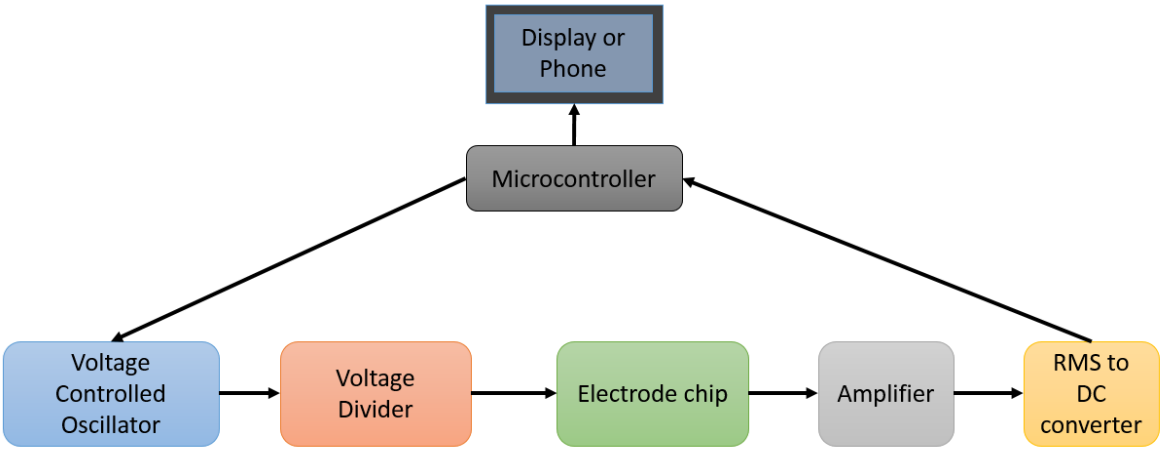

Fig 3.1: The block diagram of the overall design. The product has two parts: the electrode chip for electrochemical sensing, the circuit for the measurement, processing and display of signals.

The overall design included two main components: one was the gold electrode sensor, the other was the electrical circuit. The electrode sensor applied four two-electrode setup for EIS as the components to form a Wheatstone bridge. The microcontroller will feed a control voltage

to the voltage controlled oscillator to generate square wave of desired frequency. Then the signal generally 5 volts peak-to-peak needs to go through a voltage divider since EIS commonly applies very weak voltage of only 50 mV. Two voltages V_1 and V_2 of the Wheatstone configured electrodes will be fed to an amplifier as differential input to scale up the signals for RMS-to-DC converter (Fig 3.1). The converted RMS voltage of amplified AC signal will come back to the microcontroller which reads the input voltage as numeric value. The data will be further processed to determine whether or not targets are detected and results will be displayed on a LCD screen or in smart phone.

3.2 Electrical circuit design

The electrical circuit aims to build a primary prototype with acceptable performance. Arduino microcontroller boards are widely used as mature commercial products that provide open-source hardware and software for quick and easy circuit prototype testing. The UNO board based on ATmega328P was chosen to provide 5V power to other IC chips, control voltage to VCO and its built-in ADC could read voltage level at a rate of 10,000 times per second which was interpreted as integer values between 0 to 1023 for 0 to 5 volts. Arduino UNO provided a 5 volts power source to all the other chips and also fed into voltage divider 1 as the control voltage for VCO. Voltage Divider 1 was composed of two adjustable 10K Ohm resistor which could be used to tune the output frequency of VCO (Fig 3.2). Most voltage controller oscillators output frequency more than tens of megahertz and therefore LTC6990 was used since its output

frequency range (488 Hz to 2 MHz) was right fitted for the experiment without the need for extra frequency divider. The square wave signal from VCO needed to be attenuated by the second voltage divider since EIS generally applies only around 50 mV peak-to-peak voltage for the measurement. The attenuated signal fed into the Wheatstone bridge sensor and the two voltages was amplified as differential input to the amplifier OPA1013C. RMS-to-DC converter chip LTC1966 took the amplified AC signal and smooth it to its RMS DC signal for easier measurement. Arduino UNO could read and interpreted the DC signal as numbers. Pre-programmed codes would decide the concentration of pLDH according to the voltage reading and display corresponding diagnostic results to the LCD display or smart phone connected.

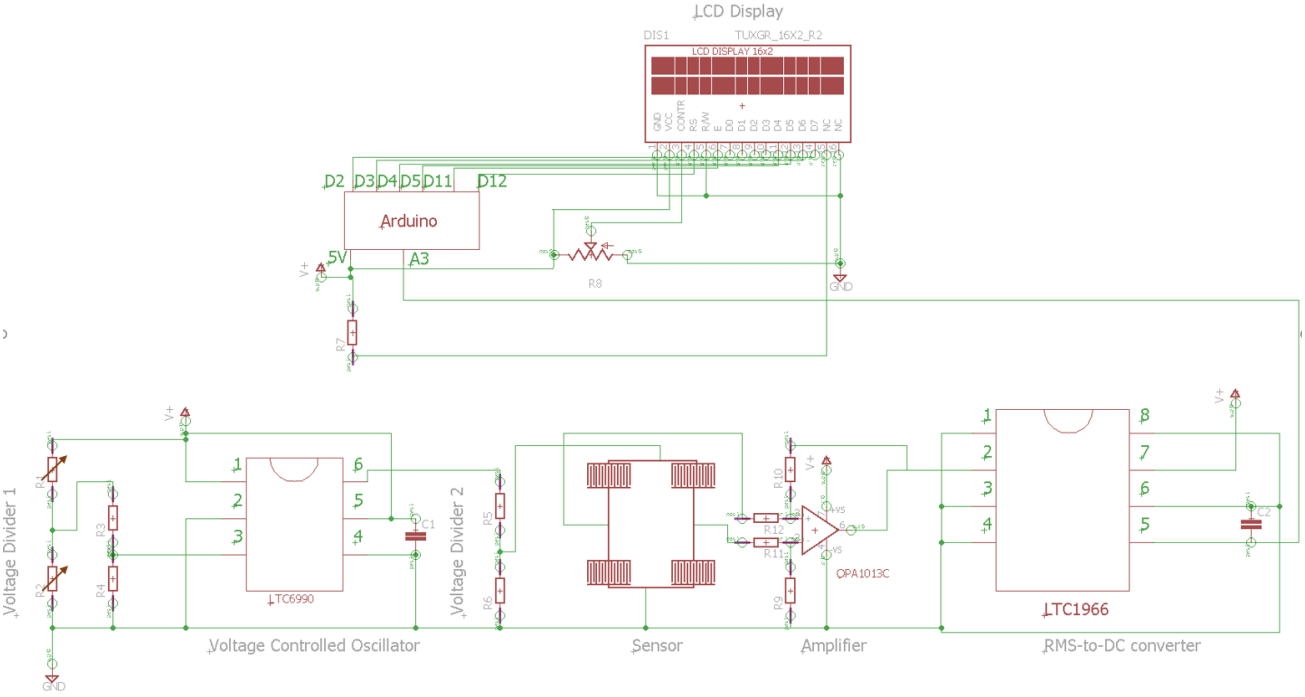

Fig 3.2: The electrical circuit schematic diagram with Arduino UNO as the microcontroller, LTC6990 as the VCO, OPA1013C as the amplifier, LTC1966 as the RMS-to-DC converter.

3.3 Sensor Specification

The gold electrode sensor was built based on printable circuit board (PCB) with two designs tested. To simplify the measurement setup, two-electrode configuration for EIS was chosen. But both electrodes were functionalized as the working electrode to increase the electrochemical impedance.

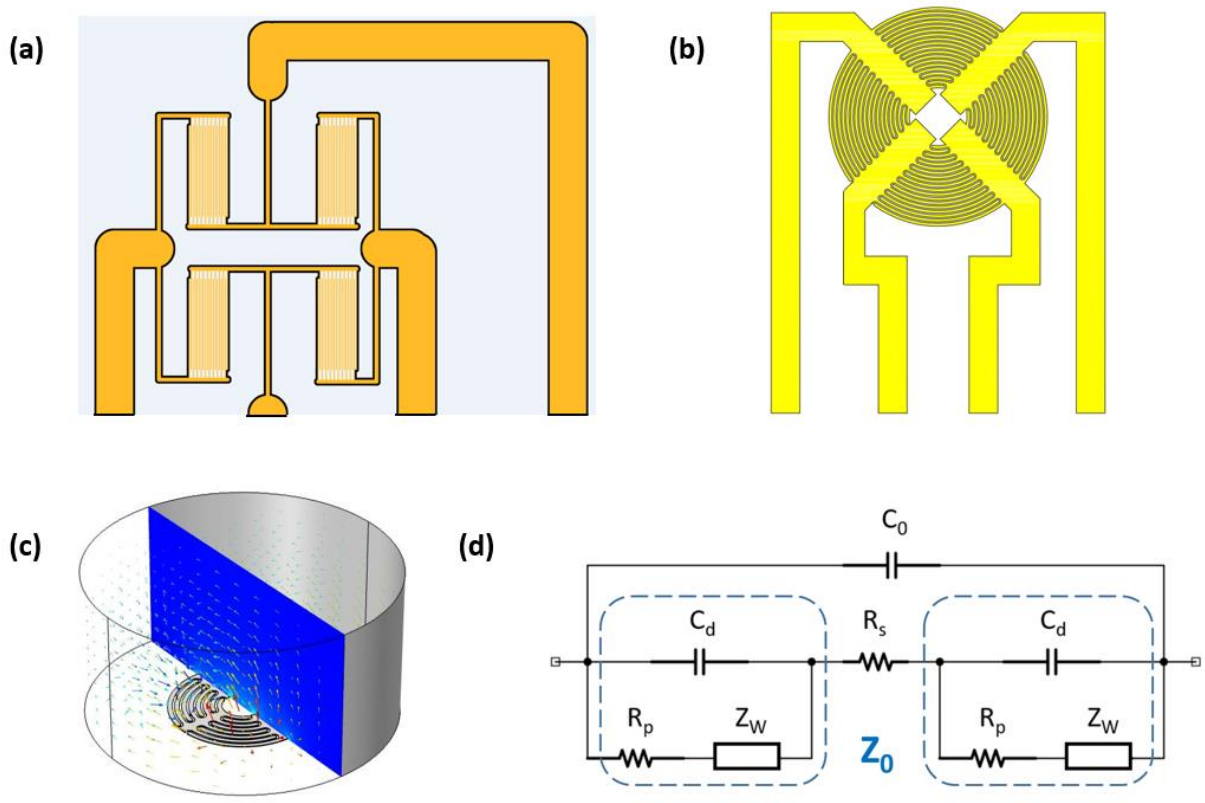

Fig 3.3: (a) First sensor design with interdigitated two-electrodes setup forming a Wheatstone bridge. (b) Second sensor design with connections of the same voltage potential merged and curved interdigitated electrodes. (c) COMSOL simulation of the second sensor. (d) Electrical equivalent circuit of two interdigitated electrodes.

Fig 3.3(a) showed the first Wheatstone sensor design made up of interdigitated electrodes. Each two nearby interdigitated electrodes formed a two-electrodes setup for EIS

measurement. There were 20 fingers for every comb-shaped electrodes with a spacing and width of 100 micron and length of 1 centimeter. The second design was similar but merged all connections of the same voltage potential together as one end (Fig 3.3(b)). All the interdigitated electrodes were curved forming a circular pattern in order to minimize the total area. Each electrode has spacing of 200 micron and width of 300 micron forming a circle of 2.3 centimeter diameter. Simulation was run in COMSOL to examine the electrical field distribution and calculated the total capacitance of the second sensor design which was 8.87 X 10^{-14} F. Attempts to simulate the effect of electrochemical impedance change by adding layers on top of electrodes was proved to be unsuccessful since lots of parameters such as the conductivity, permeability of aptamer and protein were unknown and the simulation time was very long. Therefore, the design of Wheatstone sensor could not be guided by simulation. The two designs were just prototypes tested for the purpose of optimizing protocol since results were highly unstable.

Fig 3.3(d) illustrated the electrical equivalent circuit of two interdigitated electrodes where the difference was that the counter electrode was also functionalized as working electrode. Therefore, the solution resistance R_s was followed by another set of double-layer capacitance (C_d), polarization resistance R_p and Z_w. Moreover, the two interdigitated electrodes with a gap formed a capacitor with capacitance of C_0 which was simulated in Fig 3.3(c). The impedance of C_d in parallel with R_p and Z_w was represented as Z_0 and the total impedance of two interdigitated electrodes was represented as Z_1.

$$Z_0 = \frac{R_p + Z_W}{1 + j\omega C_d (R_p + Z_W)} \quad (3)$$

$$Z_1 = \frac{R_s + 2\,Z_0}{1 + j\omega\, C_0\,(R_s + 2Z_0)} \tag{4}$$

$$= \frac{R_s + 2\big(R_p + Z_W\big) + j\omega\, R_s C_d\,(R_p + Z_W)}{1 + j\omega[\,(C_d + 2C_0)\big(R_p + Z_W\big) + C_0 R_s] - \omega^2\, C_0 C_d\, R_s (R_p + Z_W)} \tag{5}$$

$$V_{out} = V_{in}\frac{Z_1 - Z_2}{Z_1 + Z_2} = V_{in}\,\frac{Z_0}{R_s + Z_0 + j\omega\, C_0\, R_s (R_s + 2Z_0)} \tag{6}$$

$$= V_{in}\,\frac{1}{1 + 2j\omega\, C_0\, R_s + R_s(j\omega\, C_0\, R_s + 1)\dfrac{1 + j\omega\, C_d\,(R_p + Z_W)}{R_p + Z_W}} \tag{7}$$

The Wheatstone bridge had one pair of interdigitated electrodes in diagonal position coated with aptamer and then bind with pLDH while the other pair had bare gold surface. The electrical equivalent circuit of bare electrodes consisted of one C_0 in parallel with R_s which represented as $Z_2 = \frac{R_S}{1+j\omega\, C_0\, R_S}$. According to equation (2) in Chapter 2.3, the differential output voltage would be like equation (6). Since Z_W had a complex relation to frequency and could not be correctly modeled, there was no possibility to further expand equation (7). But the denominator still provided insights about the design of electrodes. For instance, a smaller R_s clearly resulted in a larger V_{out} which meant a small gap between interdigitated electrodes while keeping the electrode area constant. Although a smaller gap led to a larger C_0, the fact that C_0 was very small made it exert less dominant effect than R_s. Lacking the information of Z_w, it was hard to predict the details of how differential output voltage varied with frequency. But equation

(7) basically demonstrated a trend that as frequency went high, the denominator approached infinity resulting in V_{out} approached zero which was the same as experimental results.

3.4 Chapter summary

The purpose of this project was to innovatively convert electrochemical impedance spectroscopy to voltage measurement at different frequency which was much easier and cheaper to do. Electrical circuit was designed to replace the function of multimeter and function generator with RMS-to-DC converter and voltage controlled oscillator. The circuit also read voltages as integer numbers which could be programmed to decide infection levels and display them to a LCD display. The circuit could be made quite portable and relatively inexpensive which would be attractive for applications in remote areas. Two types of Wheatstone bridge sensor were fabricated and tested for the first phase research to examine and optimize protocols. No accurate models were available for such an electrochemical sensor and simulation was found useless. Mathematically, the electrical equivalent circuit equations provided insights of how to optimize the design. However, very limited information could be found. Therefore, the design of electrodes could only be guided through experiments.

CHAPTER 4: FABRICATION AND METHODS

4.1 Printable circuit board

4.1.1 Introduction

Printed circuit board (PCB) is widely used in today's electrical products such as smart phones, computers. Its main purpose is to mechanically secure electronic components and electrically connects them through patterned copper tracks in a compact area. PCB commonly is made of fiber glass as the substrate with copper foil bonded on to one or two sides which can be multiple layers [30].

To pattern the copper foil, several mature methods are available for fast fabrication. The most popular one is the photoengraving approach which is very similar to common MEMS fabrication technique. Firstly, PCB needs to be applied with layer of photoresist liquid or laminated with photosensitive dry film. Secondly, design the mask using CAD tools. Since most photoresist for PCB fabrication is negative, the pattern area should be white while other parts to be etched away should be black. Then the mask is placed on top of the PCB and exposed under UV light to transfer the pattern from mask to photoresist as shown in Figure 4.1(a). For negative photoresist, the exposed part will be insoluble to developer while the covered part will be removed and the photoresist can resist most etchant for copper and protect the underlying pattern (Figure 4.1(b),(c)). Finally, the board is washed in acetone or sodium hydroxide to strip remaining photoresist and the fabrication is complete.

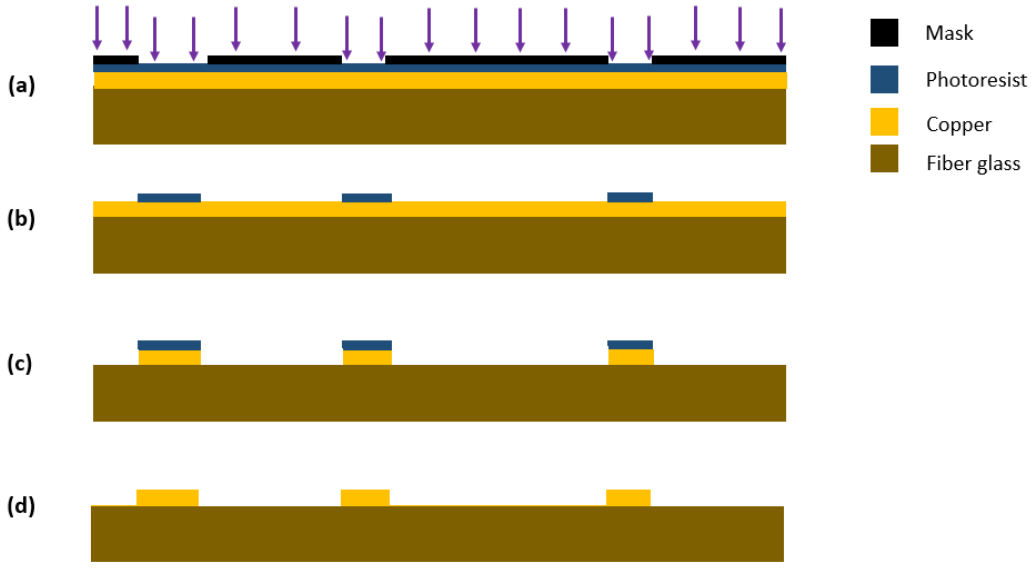

Figure 4.1: The fabrication process for PCB using the photoengraving approach. (a) UV exposure (b) Photoresist patterning (c) Etch copper (d) Dissolve remaining photoresist.

4.1.2 Fabrication

The mask was drawn in AutoCAD and export to PDF format. Since AutoCAD could not export the pattern in white color, the PDF file was modified in Adobe Photoshop to invert color and exported as BMP file. The BMP file was further modified in Adobe Illustrator to fit in letter size and saved as PDF for printing. The laser printer (Cannon D530) was compatible of 600 dpi X 600 dpi printing which meant the minimum feature it could achieve was 42.33 micron vertically and horizontally. The pattern was printed on HP transparency film for laser printer. Single layer PCB board was cut into 5cm X 5cm pieces and cleaned with soap and acetone. Photoresist dry film (INSMA) was coated on the copper surface using a thermal laminator. The board was then placed under the mask and exposed under UV light for 5 seconds using AB&M INC UV flood

exposure system. The solution of sodium carbonate was used as the photoresist developer to remove unexposed photoresist and then it was immersed into ferric chloride solution to etch the copper without photoresist on top of it. After about twenty minutes, the board was rinsed with sodium hydroxide solution to strip UV-exposed photoresist away.

4.2 Gold coating on PCB

Gold has very high electrical conductivity and excellent corrosion resistance. It has various applications in electronics mainly serve as electroplated coating on connectors and contacts [31]. There are two usual gold coating types on PCB: galvanic hard gold and flash gold. Flash gold can be obtained using two standard processes: Electroless Nickel Immersion Gold (ENIG) and electrolytic pattern plating. ENIG method first auto-catalytically deposit nickel on the palladium catalyzed copper surface and then a layer of gold is applied to nickel areas [32]. Gold flash is very thin (25-100 nm) and porous which means the underlying nickel is exposed. Obviously, flash gold is not preferred for malaria detection purpose since a constant flat gold surface is required. Galvanic hard gold coating can be achieved with very simple equipment setup and the thickness is controlled by plating current and time [32]. Figure 4.2 shows the setup for hard gold plating: the cathode of 5V DC supplier connected to the copper and the anode immersed in the plating solution without direct contact. The patterned PCB was plated with nickel first. After washing the nickel plating solution, gold layer was plated on the nickel layer using the gold plating kit (Soldertools).

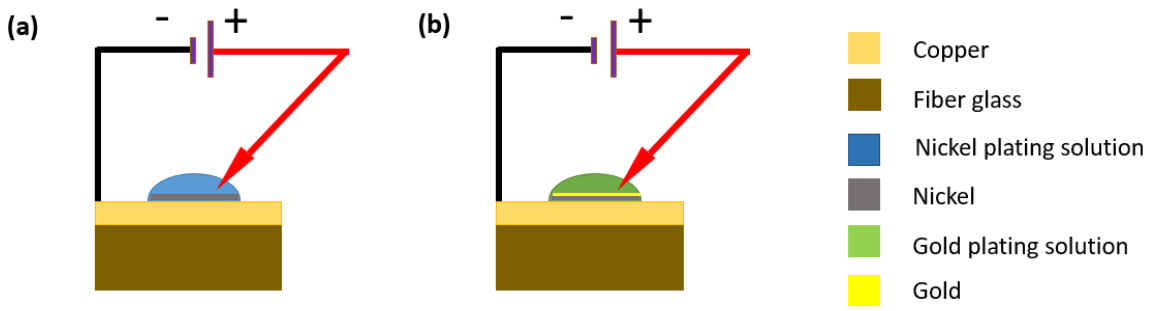

Figure 4.2: Hard gold plating for PCB diagram. (a) Nickel layer plating (b) Gold plating on nickel

4.3 Cup design

The PCB board was just one element of the sensor and it needed a cup bound to hold solution inside for functionalization and electrochemical reaction. A simple design would be cut PDMS to fit the electrodes area for primeval tests. But all electrodes were immersed in the conductive solution could lead to unwanted capacitive coupling and feed-through interference. Therefore, a better design was to have four smaller chambers for each interdigitated electrodes. Models were built in Solidworks for the first sensor design and fabricated with a 3D printer (Fig 4.3). However, the material of 3D printer was found unable to stand the cleaning process. For the second sensor design with curved fingers, a mold for 4-chambers cup was 3D printed which was then silanized for easy peeling of PDMS. Cups were glue to the PCB using PDMS and baked in 80^{o}C oven for 30 min.

4.4 Electrical circuit assembly and test

The PCB layout was designed in CadSoft Eagle and exported to PDF for printing. Fabrication process was similar to the sensor. The electrical components were soldered to the PCB and then connections to Arduino UNO were made using Dupont Cables as shown in Fig 4.3(b). The major problem of PCB was that the chip LTC6990 and LTC 1966 was very small and solder such tiny pins to PCB was very difficult. From the test result, LTC6990 had three pins shorted while LTC 1966 had four pins shorted. Another problem was that the PCB had all wires exposed where mechanical damages happened all the time result in unexpected open circuit. The whole electrical circuit was still under debugging period since most functions did not work and proper modification had been made to improve the performance.

(a) (b)

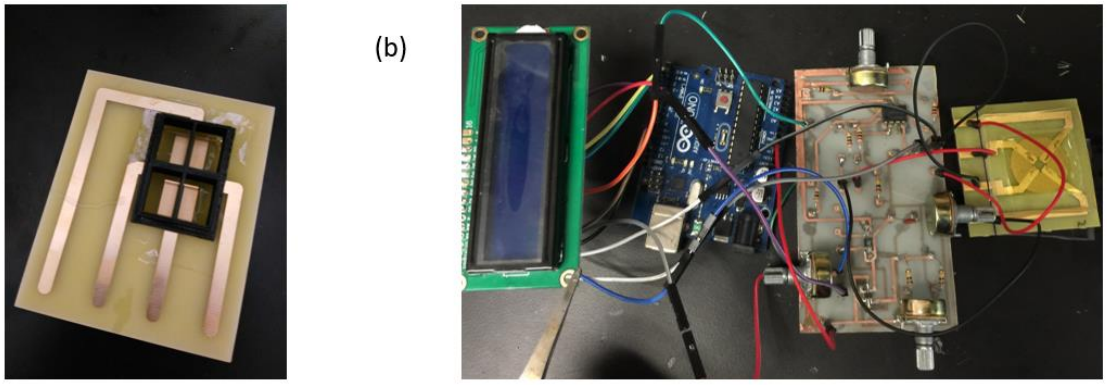

Fig 4.3: (a) First sensor design with 3D printed cup glued. (b) Electrical circuits with a LCD display, PCB connected to Arduino UNO. A curved fingers sensor bound with PDMS molded cup was connected to the PCB for input signal and measurement.

4.5 Sensor preparation

4.5.1 Gold cleaning

For electrochemical impedance spectroscopy, the quality of active gold surface will have a significant impact on measurement. Exposed to the common environment, gold surface can be contaminated by numerous ambient materials which intervene in the binding of thiols [33]. There were many cleaning methods available, of which a combination of chemical cleaning and voltammertic techniques was chosen. The gold electrodes were cleaned in hot acetone for 10 min first and then immersed into the mixture of H_2O_2 (25% v/v) and KOH (50 mM) for 10 min [34]. Finally, the electrode was applied with a potential swept from -800 to 1300 mV at a scan rate of 50 mV/s [35].

4.5.2 Gold functionalization

The aptamer needed to be thiol-modified first with TCEP (Tris[2-carboxyethyl] phosphine). For each sensor board, 10 µL apatmer stock solution (100 µM) was mixed with 40 µL TCEP (2.5 mM) for 5 hours at room temperature. Then mix the thoil-modified aptamer with 20 µL 6-mercapto-1-hexanol spacer solution in 2 mL PBS (Phosphate buffered saline) solution. To functionalize the Au surface, simply expose it to the 2 mL solution for 14 hours at room temperature [28] and rinsed it with DI water before measurement.

4.6 Experimental setup

The design of electrical circuit mainly aimed to replace the function generator and digital multimeter and construct a much cheaper and portable device. But before the circuits fully function, setup as shown in Fig 4.4 would still be used. The function generator (Agilent 33220A) would generate square wave signal with 50 mV peak-to-peak amplitude from 100 Hz to 2 MHz. The digital multimeter (Agilent 34401A) measured the voltage difference at the two ends and displayed its RMS value. Voltage measurement was performed in 5 mM $Fe(CN)_6^{3-/-4}$ with or without 1 nM pLDH. For the connection to sensor chip, Fig 4.4 (b) illustrated the detailed setup. Function generator was connected to the lowest terminal and second highest terminal. Two connectors from multimeter contacted the remaining ends. The sensor in Fig 4.4(b) had its right and left comb-shaped electrodes coated with aptamer that means a higher voltage at the second lowest terminal.

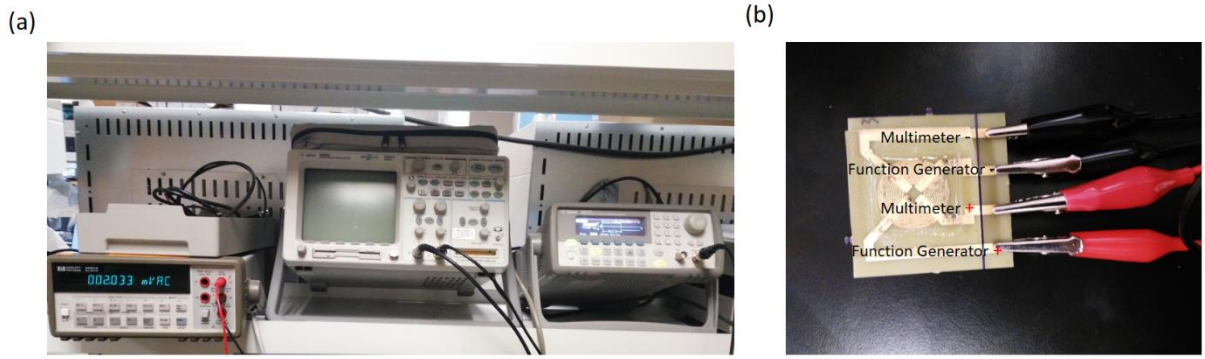

Fig 4.4: Experimental setup for voltage measurement. The function generator connected the two input ends to provide square wave signals. The digital multimeter measured the differential voltage output.

4.7 Chapter Summary

PCB fabrication technique can be used to make not only circuit board, but also any patterns satisfying design rules. PCB fabrication industry is quite mature and capable of massive production of gold coated patterns at a much lower cost, which makes it possible for commercialization. The electrical circuits have bugs to be fixed and experimental setup still needs the function generator and digital multimeter. Gold cleaning is the most critical step for stable results and further optimization will be needed for cleaning and functionalization protocols.

CHAPTER 5: RESULTS AND DISCUSSION

5.1 First design of electrodes

The first design used straight electrodes and smaller gap distance. About 90 boards were tested for verify and optimize the cleaning, functionalization and measurement protocol. The voltage differences were inconsistent with each other most times and some boards gave results that showed totally different characteristics and clearly should be ignored.

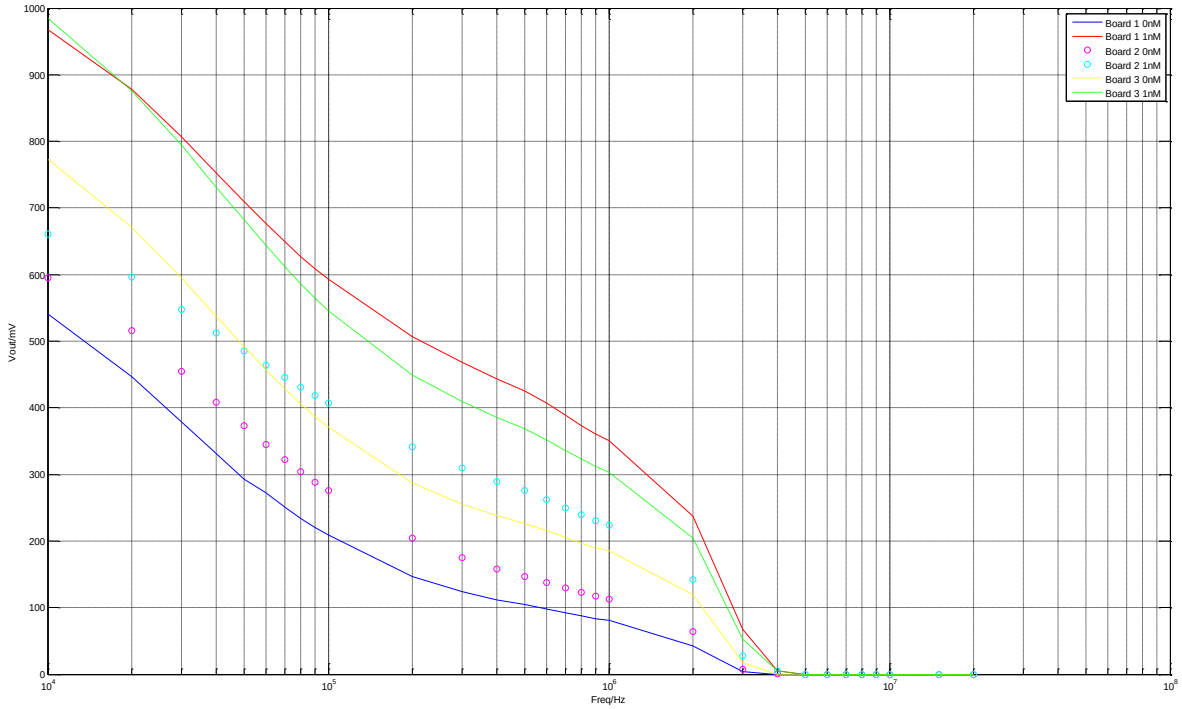

Fig 5.1: Experiment results of first sensor design. Y axis showed the RMS value of voltage difference and X axis was frequencies in logarithmic scale.

Fig 5.1 plotted the most recent results following the latest protocols from 10 KHz to 20 MHz. Two solid lines represented the resulted differential voltages of 0 nM (Blue)and 1 nM (Red) pLDH. The voltage difference kept almost constant as frequency increased until 100 KHz where it started to shrink dramatically. Similar trends could be observed from results of board 2 (dots) and 3 (dashed lines), except that they were relatively shifted upward. It was noted that the no voltages could be detected when frequency went up to around 2 MHz, which was an experimental verification of the mathematical analysis in Chapter 3.3.

5.2 Second design of electrodes

As was shown in chapter 3.3, the second type of sensors were composed of curved electrodes with a larger gap. Through experiments of first sensor, it was found that high frequency tests can be cut away since they all gave zero and lower frequencies could be explored. The new electrodes were measured from 100 Hz to 3 MHz.

Ignored the frequencies lower than 10 KHz, the plots showed similar features compared to Fig 5.1. They were all decreasing as frequency increased and the voltage difference start to significantly attenuate from around 100 KHz. When frequency went up to 2 MHz, there was almost nothing to be detected. But one major difference was that for the new curved sensor, the range voltage difference (0-350 mV) was much smaller than the first sensor (0- 950 mV). That was within expectation since the new sensor had a much larger gap between the interdigitated electrodes. By observing the low frequency part (<10 KHz), it could be seen that although there

were obvious variations, they all basically showed a trend to increase first and then decrease and the largest voltage difference could be found between 1 KHz to 3 KHz.

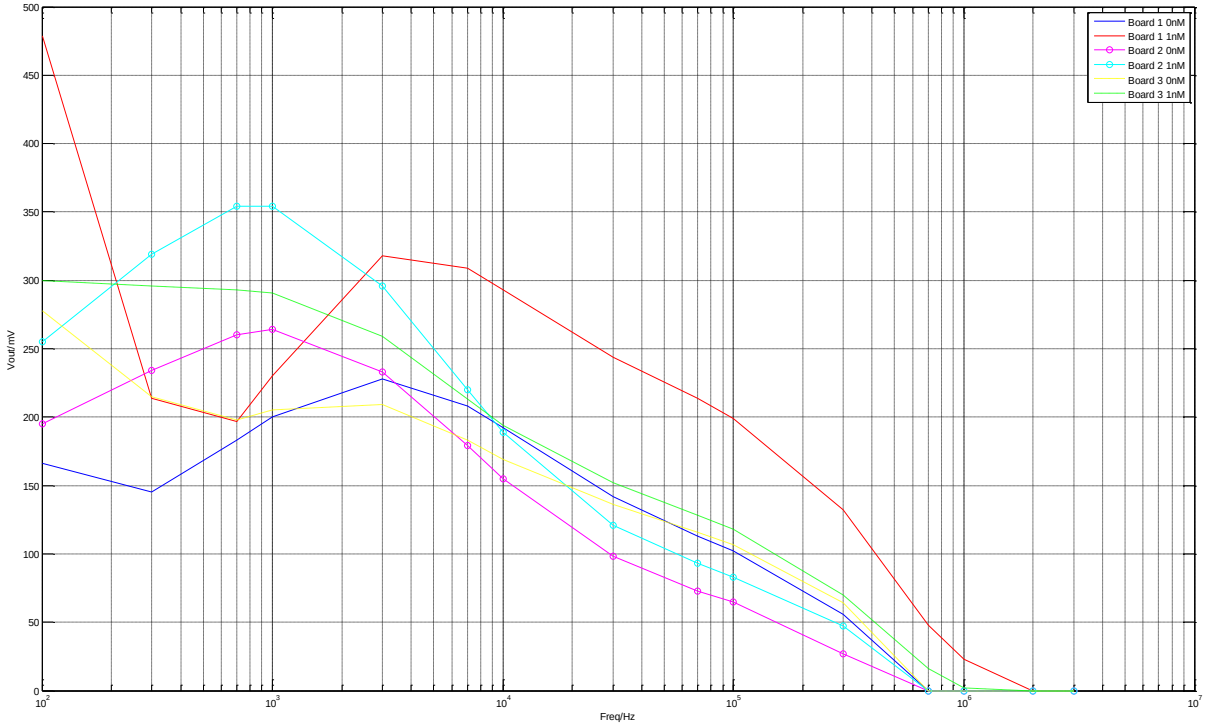

Fig 5.1: Experiment results of first sensor design. Y axis showed the RMS value of voltage difference and X axis was frequencies in logarithmic scale.

5.3 Chapter Summary

The results of both types of sensors were shown to be quite unstable. However, they still shared some characteristics that voltage differences increased a little bit first at low frequency range and started to decrease as frequency further went up. What is more, the best frequency for voltage measurement probably lay between 1-3 KHz. More importantly, the results demonstrated that the conjecture in Chapter 3.3 was correct.

CHAPTER 6: SUMMARY AND CONCLUSION

Malaria remains a serious global healthy issue especially in tropical areas even though great efforts have been made to control it. All the commercial products available for malaria detection require blood while blood drawing may lead to other infection and people with blood taboo are unwilling to provide blood. For this reason, saliva-based malaria detection has been studied and pLDH is proved to an good antigen for malaria diagnosis.

Electrochemical impedance spectroscopy is a very old but powerful detection method which demonstrate an extensive application for biological purpose. Studies have shown that EIS can have great sensitivity and specificity for the detection of various proteins, DNAs and even bacteria. However, common EIS run tests over a wide frequency range and requires cumbersome machines. Therefore, the idea of applying Wheatstone bridge to convert electrochemical impedance into differential voltages comes up to diagnose pLDH concentration.

6.1 Overall evaluation of current work

Current work demonstrates the feasibility of building an electrochemical sensor that can convert impedance variation to voltage difference and constructing portable electrical circuits for measurement purpose. Through one year's efforts of information accumulation and testing, a mature protocol for cleaning, functionalization and sensor fabrication is confirmed. Lots of innovative solutions has been generated to solve all the engineering problems coming up.

However, both the sensor and the electrical circuit have issues that need to be resolved. A stable result from the sensor is critical and tons of works are still required to figure everything out. For the electrical circuit, problems appeared are quite clear and only careful debugging is needed. In conclusion, current work finishes the first phase of the whole research that theoretical ideas are tested and proved.

6.2 Future work

The future work will still focus on how to improve the stability of results that means continuous modification of cleaning, functionalization protocols. After satisfying results can be obtained, fundamental researches on sensor design will be performed. Different parameters including electrode dimension, gaps in between, will be tested to find out the optimized design. Electrical circuits also need to be debugged and modified in order to demonstrate the possibility of building a portable device. The next phase will be cutting the costs. For electrode sensor, studies on what is the smallest amount of chemicals to achieve acceptable results will be performed. The electrical circuit can also be made cheaper by choosing other electrical components.

REFERENCES

1. WHO: World Health Organization: World malaria report. Geneva 2015.

2. Idro, R., Marsh, K., John, C. C., & Newton, C. R. J. (2010). Cerebral malaria: Mechanisms of brain injury and strategies for improved Neurocognitive outcome. Pediatric Research, 68(4), 267–274.

3. Fleischer, B. (2004). Editorial: 100 years ago: Giemsa's solution for staining of plasmodia. Tropical Medicine and International Health, 9(7), 755–756.

4. Anchinmane, V. T., & Shedge, R. T. (2011). A Review of Malaria Diagnostic Tools: Microscopy and Rapid Diagnostic Test. Asian Journal of Medical Sciences Asian J Med Sci, 1(2).

5. Bejon, P., Andrews, L., Hunt-Cooke, A., Sanderson, F., Gilbert, S. C., Hill, A. V. (2006). Thick blood film examination for Plasmodium falciparum malaria has reduced sensitivity and underestimates parasite density. Malaria Journal, 5(104).

6. Moody, A., Hunt-Cooke, A., Gabbett, E., & Chiodini, P. (2000). Performance of the optiMAL malaria antigen capture dipstick for malaria diagnosis and treatment monitoring at the hospital for tropical diseases, London. SHORT REPORT. *British Journal of Haematology*, *109*(4), 891–894.

7. Miller, R. S., Mcdaniel, P., & Wongsrichanalai, C. (2001). Following the course of malaria treatment by detecting parasite lactate dehydrogenase enzyme. British Journal of Haematology Br J Haematol, 113(2), 558-562.

8. Research, G. V. (2016). *Malaria diagnostics market size | industry report, 2022*. Retrieved May 13, 2016, from http://www.grandviewresearch.com/industry-analysis/malaria-diagnostics-market

9. Lima, D. P., Diniz, D. G., Moimaz, S. A. S., Sumida, D. H., & Okamoto, A. C. (2010). Saliva: Reflection of the body. *International Journal of Infectious Diseases*, *14*(3), e184–e188.

10. Wilson, N., Adjei, A., Anderson, W., Baidoo, S., Stiles, JK. (2008). Short report: Detection of *Plasmodium falciparum* histidine-rich protein II in saliva of malaria patients. *Am J Trop Med Hyg*, 78(5), 733–735.

11. Fung, A. O., Damoiseaux, R., Grundeen, S., Panes, J. L., Horton, D. H., Judy, J. W., & Moore, T. B. (2012). Quantitative detection of PfHRP2 in saliva of malaria patients in the Philippines. Malar J Malaria Journal, 11(1), 175.

12. Gbotosho, G. O., Happi, C. T., Folarin, O., Keyamo, O., Sowunmi, A., & Oduola, A. M. J. (2010). Rapid detection of lactate Dehydrogenase and Genotyping of plasmodium falciparum in saliva of children with acute uncomplicated malaria. American Journal of Tropical Medicine and Hygiene, 83(3), 496–501.

13. Mharakurawa, S., Simoloka, C., Thuma, P. E., Shiff, C. J, Sullivan, D. J (2006).Detection of Plasmodium falciparum, wilsonPCR detection of Plasmodium falciparum in human urine and saliva samples. Malaria Jouranls, 5(103).

14. Nwakanma, D., Gomez‐Escobar, N., Walther, M., Crozier, S., Dubovsky, F., Malkin, E., . . . Conway, D. (2009). Quantitative Detection of Plasmodium falciparum DNA in Saliva, Blood, and Urine. The Journal of Infectious Diseases J INFECT DIS, 199(11), 1567-1574.

15. Singh, R., Singh, D. P., Gupta, R., Savargaonkar, D., Singh, O. P., Nanda, N., . . . Valecha, N. (2014). Comparison of three PCR-based assays for the non-invasive diagnosis of malaria: Detection of Plasmodium parasites in blood and saliva. Eur J Clin Microbiol Infect Dis European Journal of Clinical Microbiology & Infectious Diseases, 33(9), 1631-1639.

16. Macdonald, D. D. (2006). Reflections on the history of electrochemical impedance spectroscopy. Electrochimica Acta, 51(8-9), 1376–1388.

17. Chang, B., Park, S. (2010). Electrochemical Impedance Spectroscopy. Annual Review of Analytical Chemistry, 3, 207 -229.

18. Lvovich, V. F. (2012). Impedance spectroscopy: Applications to electrochemical and dielectric phenomena. Hoboken, NJ: Wiley.

19. Lasia, A. (2014). Electrochemical impedance spectroscopy and its applications.

20. Ganesh, V., Pandey, R. R., Malhotra, B., & Lakshminarayanan, V. (2008). Electrochemical characterization of self-assembled monolayers (SAMs) of thiophenol and aminothiophenols on polycrystalline Au: Effects of potential cycling and mixed SAM formation. Journal of Electroanalytical Chemistry, 619-620, 87-97.

21. Berggren, C., Bjarnason, B., & Johansson, G. (2001). Capacitive Biosensors. Electroanalysis, 13(3), 173–180.

22. Yeo, J., Park, J.-Y., Bae, W. J., Lee, Y. S., Kim, B. H., Cho, Y., & Park, S.-M. (2009). Label-free Electrochemical detection of the p53 core domain protein on its antibody immobilized electrode. Analytical Chemistry, 81(12), 4770–4777.

23. Tsekenis, G., Garifallou, G.-Z., Davis, F., Millner, P. A., Gibson, T. D., & Higson, S. P. J. (2008). Label-less Immunosensor assay for Myelin basic protein based upon an ac Impedance protocol. Analytical Chemistry, 80(6), 2058–2062.

24. Maalouf, R., Fournier-Wirth, C., Coste, J., Chebib, H., Saïkali, Y., Vittori, O., … Jaffrezic-Renault, N. (2007). Label-free detection of bacteria by Electrochemical Impedance spectroscopy: Comparison to surface Plasmon resonance. Analytical Chemistry, 79(13), 4879–4886.

25. Qiu, Y., Liao, R., & Zhang, X. (2009). Impedance-Based monitoring of ongoing Cardiomyocyte death induced by tumor necrosis Factor-α. Biophysical Journal, 96(5), 1985–1991.

26. Drummond, T. G., Hill, M. G., & Barton, J. K. (2004). Electrochemical DNA sensors. ChemInform, 35(27).

27. Nimjee, S. M., Rusconi, C. P., & Sullenger, B. A. (2005). Aptamers: An emerging class of Therapeutics. *Annual Review of Medicine*, *56*(1), 555–583.

28. Lee, S., Song, K.-M., Jeon, W., Jo, H., Shim, Y.-B., & Ban, C. (2012). A highly sensitive aptasensor towards plasmodium lactate dehydrogenase for the diagnosis of malaria. Biosensors and Bioelectronics, 35(1), 291–296.

29. Hoffmann, K. (1974). Applying the Wheatstone bridge circuit. Darmstadt: HBM.

30. Ho, W., & Ji, P. (2006). Optimal production planning for PCB assembly. United Kingdom: Springer London.

31. Goodman, P. (2002). Current and future uses of gold in electronics. Gold Bulletin, 35(1), 21–26.

32. Le Solleu, J. . (2010). Sliding contacts on printed circuit boards and wear behavior. The European Physical Journal Applied Physics, 50(1), 12902.

33. Fischer, L. M., Tenje, M., Heiskanen, A. R., Masuda, N., Castillo, J., Bentien, A., … Boisen, A. (2009). Gold cleaning methods for electrochemical detection applications. Microelectronic Engineering, 86(4-6), 1282–1285.

34. Heiskanen, A. R., Spégel, C. F., Kostesha, N., Ruzgas, T., & Emnéus, J. (2008). Monitoring of Saccharomyces cerevisiae cell proliferation on Thiol-Modified planar gold Microelectrodes using Impedance spectroscopy. Langmuir, 24(16), 9066–9073.

35. Min, K., Cho, M., Han, S.-Y., Shim, Y.-B., Ku, J., & Ban, C. (2008). A simple and direct electrochemical detection of interferon-γ using its RNA and DNA aptamers. Biosensors and Bioelectronics, 23(12), 1819–1824.